BU-CCS-990401

LA-UR 00-118

Fourier Acceleration of Langevin Molecular Dynamics

Francis J. Alexander

CIC-3, MS-B256, Los Alamos National Laboratory, University of California

Los Alamos, New Mexico 87545

fja@lanl.gov

Bruce M. Boghosian and Richard C. Brower

Center for Computational Science and Department of Physics, Boston University,

3 Cummington Street, Boston, Massachusetts 02215

bruceb@bu.edu and brower@bucrf20.bu.edu

S. Roy Kimura

Department of Biomedical Engineering, Boston University,

Boston, Massachusetts 02215

srk@engc.bu.edu

February 1, 2008

Abstract

Fourier acceleration has been successfully applied to the simulation of lattice field theories for more than a decade. In this paper, we extend the method to the dynamics of discrete particles moving in continuum. Although our method is based on a mapping of the particles' dynamics to a regular grid so that discrete Fourier transforms may be taken, it should be emphasized that the introduction of the grid is a purely algorithmic device and that no smoothing, coarse-graining or mean-field approximations are made. The method thus can be applied to the equations of motion of molecular dynamics (MD), or its Langevin or Brownian variants. For example, in Langevin MD simulations our acceleration technique permits a straightforward spectral decomposition of forces so that the long-wavelength modes are integrated with a longer time step, thereby reducing the time required to reach equilibrium or to decorrelate the system in equilibrium. Speedup factors of up to 30 are observed relative to pure (unaccelerated) Langevin MD. As with acceleration of critical lattice models, even further gains relative to the unaccelerated method are expected for larger systems. Preliminary results for Fourier-accelerated molecular dynamics are presented in order to illustrate the basic concepts. Possible extensions of the method and further lines of research are discussed.

1 Introduction

Molecular dynamics (MD) simulations play an important role in our fundamental understanding of the kinetics of molecular systems and provide a powerful tool for modeling a wide variety of materials including biomolecules. Although MD simulations have benefited tremendously from advances in high-performance computing, they suffer from the limitation arising from the numerical stiffness inherent in Newton's equations. The result is that MD studies are generally restricted to short intervals of real time, from nanoseconds up to a few microseconds, even with heroic computational efforts. To overcome this difficulty, there is a growing effort to develop accelerated MD algorithms. (See, for example, [1, 2, 3, 4, 5, 6].)

In contrast to molecular (or other discrete particle) systems with a Lagrangian data representation, there is a considerable variety of acceleration algorithms available for continuum field theories approximated on a regular grid or lattice. For example, grid-based simulations have made substantial progress with the advent of cluster Monte Carlo methods [7, 8], Fourier acceleration [9], and multi-grid iterative solvers [10]. Because the bulk properties of large aggregates of molecules can often be described by continuum mechanics, it is intuitively appealing that a corresponding method should apply in the molecular (or particulate) framework. Indeed, making this connection between the molecular and continuum scales is a central goal for multi-scale modeling projects. In this paper we show how one such continuum tool, namely Fourier acceleration, can be applied to Langevin MD without introducing any coarse-graining or mean-field approximations. The basic ingredient of the method is an exact mapping of the original particulate system onto a regular lattice of displacement fields. Although this mapping may prove useful in a broader context, we restrict our attention to Fourier acceleration of the Langevin equations for MD.

The idea of introducing a regular grid into MD is not new; grid-based recursive multipole expansions [11], for example, have been used for more than a decade to rapidly compute Coulomb interactions. More recently, hybrid atomistic-continuum techniques, such as the quasi-continuum method [12], use finite-element techniques to bridge microscopic and macroscopic length scales. Most applications of spectral methods to molecular systems, however, have been confined to the analysis of data (for example, structure and response functions).

By contrast, our procedure uses spectral analysis to modify and accelerate the dynamical evolution of the molecular system. Unique to this approach is the mapping of the actual position coordinates to a grid, and the ability to invert the mapping to displace the original off-lattice molecular coordinates. The introduction of the grid is a purely algorithmic device and is not tantamount to a coarse-graining or mean-field approximation of any kind; that is, the accelerated dynamics are still those of discrete particles. The result is a new, accelerated, stochastic dynamics that is significantly faster than standard Langevin MD, but still exactly preserves the equilibrium distribution. The fundamental tradeoff associated with this approach is that of speed versus faithfulness to the essential kinetics. Both of these desiderata are clearly specific to the system being studied and the phenomena that the model should faithfully represent.

The organization of this paper is as follows. Section 2 describes our procedure for mapping the particulate system to a regular lattice. This mapping is a prerequisite to the application of a Fourier-mode decomposition. In Section 3 we outline the Fourier-accelerated Langevin dynamics on the grid. We demonstrate the method in Section 4 by applying it to a ϕ^4 model at its critical point. We then describe how to apply Fourier acceleration (FA) in conjunction with the lattice mapping in Section 5. As an example, in Section 6, we apply the method to the Langevin dynamics of a simple Lennard-Jones fluid. Extensions of the Fourier-accelerated molecular dynamics (FAMD) method and additional applications are discussed in Section 7.

2 Particle-to-Grid Mapping Procedure

There are many ways by which a molecular system can be transformed from (off-lattice) particle coordinates to a fiducial grid. Each has its advantages and disadvantages, depending upon the aim of the transformation. In this section we discuss one method that has proven to be particularly useful.

In one dimension, the simplest mapping procedure procedure is to sort the particles by their position coordinate. Each particle i is given a permuted label $n(i)$ so that $n(i) < n(j)$ if $x_i < x_j$. Whereas the i and j indices are arbitrary labels, devoid of physical significance, the permuted labels are based on the sequence of particle positions and hence may be thought of as lying on a grid with some physical meaning. Because $n(i)$ is a permutation, it has inverse function $i(n)$ such that $n(i(\cdot)) = \cdot$. We now transform to new coordinates by the prescription $X_n = x_{i(n)}$. This mapping makes it possible to directly Fourier transform the new position coordinates,

$$\tilde{X}_k = \frac{1}{L} \sum_n X_n e^{ikn}. \tag{2.1}$$

Note that this new spatial representation contains precisely the same amount of information as the original data. Also note that because this mapping is merely a geometrically motivated relabeling, all attributes, such as mass m_i, are automatically transfered to the new representation.

The multidimensional generalization of this method is not so straightforward. The problem of sorting the particles in more than one dimension is not well defined. There is, however, a very good and efficient approximation used by numerical analysts for load-balancing graphs on multiprocessor architectures, known as *Recursive Coordinate Bisection* (RCB) [13]. To see how this algorithm works, consider a two-dimensional square domain containing $N = L^2$ particles, where L is a power of 2. We first introduce a two-index label $\mathbf{i} = (i_x, i_y)$ for the particles, where

$$i_x(i) = i \bmod L \tag{2.2}$$

$$i_y(i) = (i - i_x)/L, \tag{2.3}$$

so that

$$i(\mathbf{i}) = i_x + (i_y - 1)L. \tag{2.4}$$

Thus the transformation from one-index labels i to two-index labels $\mathbf{i}$ is a bijection. We can label the particles' coordinates as $\mathbf{x}_i = (x_i, y_i)$, or equivalently as $\mathbf{x}_\mathbf{i} = (x_\mathbf{i}, y_\mathbf{i}) = (x_{i(\mathbf{i})}, y_{i(\mathbf{i})})$. as with the i labels for the one-dimensional case, these labels (both i and $\mathbf{i}$) are assigned arbitrarily and devoid of physical content.

Whereas it is difficult to see how to order the one-index labels i, the RCB method provides a straightforward prescription for permuting the two-index labels $\mathbf{i}$ into a new set of two-index labels $\mathbf{n}(\mathbf{i})$ that are based on the particles' positions. Again, this function is a permutation, so it has an inverse $\mathbf{i}(\mathbf{n})$, such that $\mathbf{n}(\mathbf{i}(\cdot)) = \cdot$. The $\mathbf{n}$'s may reasonably be taken to lie on a regular two-dimensional grid, and hence provide a set of independent variables with respect to which the new coordinates $\mathbf{X}_\mathbf{n} \equiv \mathbf{x}_{\mathbf{i}(\mathbf{n})} = \mathbf{x}_{i(\mathbf{i}(\mathbf{n}))}$ can be Fourier transformed, just as in the one-dimensional example.

To accomplish this, the physical domain is first divided into left- and right-hand portions with equal numbers ($N/2$) of particles, by sorting the particles on their x coordinates. The half with smaller x coordinates will have $1 \le n_x \le L/2$ and the half with larger x coordinates will have $L/2 < n_x \le L$. In binary notation, this labeling sets the most significant bit of the n_x index to

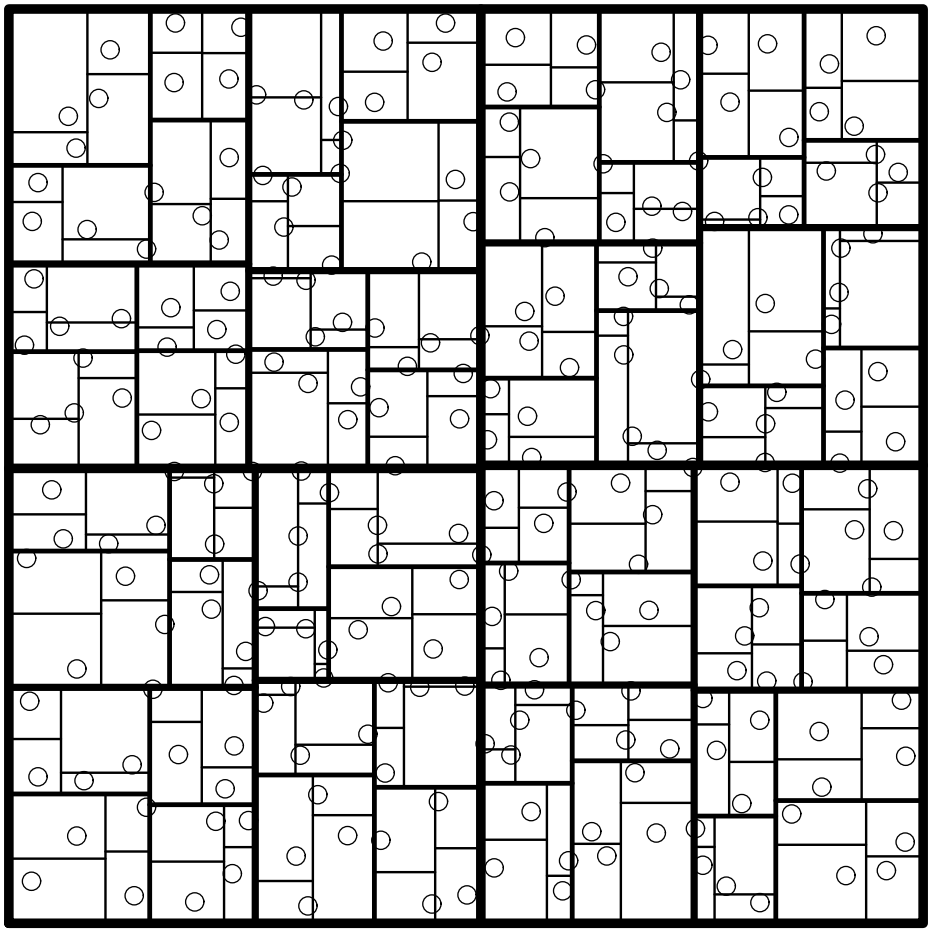

Figure 1: Grid Mapping for a two-dimensional Lennard Jones fluid by Recursive Coordinate Bisection.

zero/one for the left/right halves. Next, we sort each set of $N/2$ particles by their y coordinates to obtain 4 sets of $N/4$ particles, likewise setting the most significant bit in the n_y. This procedure is then applied recursively to each of the 4 boxes with $N/4$ particles, maintaining the alternation between the x and y axes. For systems of relatively uniform density, the resulting fiducial grid leads to a remarkably regular and local particle-labelling scheme. RCB is an order $N \log N$ algorithm with many obvious similarities to fast Fourier transforms.

3 Fourier Accelerated Langevin Dynamics

To demonstrate how Fourier Acceleration works, we consider in detail a simple (discrete-time) Langevin dynamics. The Langevin equation of motion for a system of N particles is

$$\mathbf{x}_i(t + \Delta t) = \mathbf{x}_i(t) + \frac{\mathbf{f}_i(t)}{2m_i} (\Delta t)^2 + \mathbf{p}_i(t)\Delta t, \tag{3.1}$$

where the N momenta are Gaussian random variables $\langle \mathbf{p}_i(t)\mathbf{p}_j(t')\rangle = \frac{1}{2}k_B T m_i \delta_{i,j}\delta_{t,t'}\mathbf{1}$. It is well known that this dynamics (in the limit of vanishing time step) samples the canonical-ensemble

Boltzmann-Gibbs equilibrium distribution function,

$$P(\mathbf{x}_i, \mathbf{p}_i) = \frac{1}{Z} \exp\left[-\beta\left(\frac{\beta p_i \cdot p_i}{2m_i} + V(\mathbf{x}_i)\right)\right], \tag{3.2}$$

where $\beta \equiv 1/k_B T$ and the force is $f_i = -\partial V/\partial \mathbf{x}_i$.

For the moment, we set this result aside and consider lattice field problems for which Batrouni et al. [9] have shown how to accelerate the approach to equilibrium in Fourier space. For example, consider fields $\phi_{\mathbf{x}}(t)$ on a uniform grid with sites $\mathbf{x}$, obeying the equilibrium distribution,

$$P(\phi_{\mathbf{x}}) = \frac{1}{Z} e^{-S(\phi_{\mathbf{x}})} \tag{3.3}$$

with action S. This distribution is a fixed point of the discrete Langevin dynamics (as $\Delta t \to 0$),

$$\phi_{\mathbf{x}}(t + \Delta t) = \phi_{\mathbf{x}}(t) - K \frac{\partial S(\phi_{\mathbf{x}})}{\partial \phi_{\mathbf{x}}} (\Delta t)^2 + \eta_{\mathbf{x}}(t) \Delta t \ , \tag{3.4}$$

where $\eta_{\mathbf{x}}(t)$ are Gaussian random fields. This Markov process, however, is not the only one which drives the system to the equilibrium in Eq. (3.3). Indeed, the local dynamics of Eq. (3.4) generally exhibits long autocorrelation times near critical points. Batrouni et al. [9] have shown how to accelerate such grid-based Langevin equations using a Fourier decomposition of the dynamics. The Fourier Acceleration (FA) method depends on the simple observation that *any* mobility (or inverse mass) matrix may be introduced by the substitutions, $K \to K_{\mathbf{x},\mathbf{x}'}$ and $\langle \eta_{\mathbf{x}}(t) \eta'_{\mathbf{x}}(t) \rangle = K_{\mathbf{x},\mathbf{x}'} \delta(t', t) \mathbf{1}$, without upsetting the equilibrium distribution of the fields. One such choice is a matrix K which is diagonal in Fourier space. This choice leads to acceleration if the time steps for the slow (low wavenumber) modes are amplified.

$$\phi_{\mathbf{x}}(t + \Delta t) = \phi_{\mathbf{x}}(t) + \mathcal{F}^{-1}\left[-\tilde{K}(\mathbf{k}) \mathcal{F}\left[\frac{\partial S}{\partial \phi_{\mathbf{x}}}\right] (\Delta t)^2 + \sqrt{\tilde{K}(\mathbf{k})}\ \eta_{\mathbf{k}}\ \Delta t\right], \tag{3.5}$$

where $\mathcal{F}$ represents a Fourier transform. A simple substitution of the field $\phi_{\mathbf{x}}$ with the position of a particle $\mathbf{x_i}$ would allow us to use Fourier methods. The mappings of Sec. 2 provide that substitution.

4 ϕ^4 Model

To illustrate the above procedure we apply the FA technique to the ϕ^4 model at the critical point in two dimensions. It has been shown by Batrouni *et al.* [9] that critical slowing down is completely eliminated by FA in a purely Gaussian model. Of course, in that case, the modes completely decouple in momentum space and each can be integrated independently. For a nonlinear model with mode-coupling, it is not guaranteed that FA will work at all. It is also not clear *a priori* what the optimal choice of the mass matrix should be that will most rapidly drive the system to equilibrium or decorrelate the system once in equilibrium.

To gain experience in selecting the mass matrix for FAMD, we first studied a simpler system, namely the ϕ^4 model in two dimensions at criticality. This model provides a qualitative (and in some cases quantitative) description of a displacive phase transition. The investigation of such transitions is one of our long-term goals. Surprisingly, the FA method applied to this system at its critical point has not been analyzed. However, Batrouni and Svetitsky have studied its application

to first-order phase transitions in a ϕ^4 model and found a significant speedup of tunneling between minima [14].

The Hamiltonian is given by,

$$\begin{aligned} \beta\mathcal{H}([\phi]) &= \sum_{i=1}^{N}\left[\frac{-\theta}{2}\phi_i^2+\frac{\chi}{4}\phi_i^4+\frac{1}{2}\sum_{\mu=1}^{d}\left(\phi_{i_\mu}-\phi_i\right)^2\right] \\ &= \sum_{i=1}^{N}\left[\frac{\tilde{\theta}}{2}\phi_i^2+\frac{\chi}{4}\phi_i^4-\frac{1}{2}\sum_{\mu=1}^{2d}\phi_i\phi_{i_\mu}\right], \end{aligned} \tag{4.1}$$

where

$$\tilde{\theta} = 2d-\theta \ . \tag{4.2}$$

This system exhibits critical behavior along a line of critical parameters, χ and θ. We simulated the system at the critical point, $\chi = 1.0$, $\theta = 1.265$, which was numerically determined previously by Toral and Chakrabarti [18].

We updated this system using the Fourier accelerated Langevin equation described above, namely,

$$\phi_i(t+\Delta t) = \phi_i(t)+\mathcal{F}^{-1}\left[K(\mathbf{k})\mathcal{F}\left(-\frac{\delta\mathcal{H}}{\delta\phi}\right)+\sqrt{k_BT\ K(\mathbf{k})}\ \tilde{\eta}(\mathbf{k})\right], \tag{4.3}$$

where $\tilde{\eta}(\mathbf{k})$ represents the Fourier transformed Gaussian noise with $\langle\eta\rangle = 0$ and $\langle\eta^2\rangle = 1$, and $K(\mathbf{k})$ represents the mass matrix which gives us the desired acceleration. We chose the mass matrix to be the lattice propagator of the free theory,

$$K(\mathbf{k}) = \frac{4d+m^2}{4\sum_{\mu=1}^{d}\sin^2\frac{k_\mu}{2}+m^2}\ (\Delta t)^2\ , \tag{4.4}$$

where the parameter m is expected to be order $1/\xi$ or $1/L$ for finite-size scaling [9]. The value of this parameter was adjusted during trial simulations by setting $m = c/L$ for different values of the constant c. We report the results for $c = 4\sqrt{2}$. As a check, we repeated the simulations without Fourier acceleration using the pure Langevin update,

$$\phi_i(t+\Delta t) = \phi_i(t)+\frac{\Delta t^2}{2}f(\phi)+\sqrt{k_BT}\ \eta, \tag{4.5}$$

where η is a zero-mean unit-variance Gaussian random variable and the force term, $f(\phi)$, is,

$$f(\phi) = -\frac{\delta\mathcal{H}}{\delta\phi} = -\sum_{i=1}^{N}\left(\tilde{\theta}\phi_i-\chi\phi_i^3-\sum_{\mu=1}^{2d}\phi_{i_\mu}\right). \tag{4.6}$$

Finite-size scaling simulations were conducted for $L\times L$ system sizes where $L = 2$, 4, 8, 16, 32, 64 using the FA Langevin update and for $L = 2$, 4 , 8, 16 for the pure Langevin case. A time step of $\Delta t = 0.05$ was used. Note that our time step corresponds to $\sqrt{\epsilon}$ in Ref. [9] and thus should give very little discretization error. We ran each system for time that is approximately 1000 times longer the correlation time estimated from trial simulations. The results are shown in Fig. 2. The normalized correlation functions, $C(t) = \langle E(0)E(t)\rangle/\langle E(0)E(0)\rangle$, were computed from the time series of the energy density. Correlation times τ for each L were computed by fitting the region $0.3 \le C(t) \le 0.6$ to $\exp(-t/\tau)$. Error bars were estimated from the standard deviation of the

System Size	Heat bath		Langevin		FA	
	Value	Error	Value	Error	Value	Error
$L = 2$	0. 481	± 0. 0159	0. 496	± 0. 0612	0. 473	± 0. 0432
$L = 4$	3. 174	± 0. 0411	3. 180	± 0. 4019	3. 291	± 0. 2998
$L = 8$	14. 54	± 0. 1576	14. 65	± 0. 9797	14. 87	± 0. 5239
$L = 16$	61. 16	± 0. 4790			62. 58	± 1. 6278
$L = 32$	251. 5	± 1. 6066			260. 6	± 3. 5662

Table 1: Mean energies and errors for each system size and update method. Errors are standard deviations from 10 blocked averages.

values of τ measured from five independent time series per system. Average energies and standard deviations of 10 blocked averages were measured for each system size and update algorithm. These results are listed in Table 1.

In Fig. 2 we compare the autocorrelation times for the pure Langevin update with those for the Fourier-Langevin case. There is clearly an acceleration. Whether the dynamical exponent z, which describes the growth of autocorrelation times by the scaling relation, $\tau = L^z$, is actually different for Langevin and Fourier Acceleration is an interesting and open question, and would require more extensive computation than we have done to date. For practical simulations of systems far from criticality, the value of z is often not as important as the overall amplitude of the autocorrelation time.

5 Fourier Accelerated Molecular Dynamics

To apply these techniques to discrete particles with a Lagrangian data representation, we must introduce a Fourier transform of the position coordinates $\mathbf{x}_i(t)$. Clearly we cannot simply transform the $\mathbf{x}_i$ with respect to the particle labels $i = 1, 2, \ldots N$. As mentioned in Sec. 2, these labels are generally devoid of physical meaning. They have no natural relationship to the properties of the particles or to their spatial and/or temporal configuration. Hence, the first step is to map the particles onto a uniform spatial grid.

The mapping scheme discussed in Sec. 2 suggests how to define appropriate grid coordinates. In the Index Method, the mapping, $\mathbf{x}_i \rightarrow \mathbf{X}_\mathbf{n}$, is simply a relabling of the coordinates. (To be more explicit this notation for a 2D system is expanded into components: $\mathbf{x}_i \equiv (x_i, y_j)$ and $\mathbf{X}_\mathbf{n} = (X_{n_x,n_y}, Y_{n_x,n_y})$, where $\mathbf{n} = (n_x, n_y)$ is a two component integer vector.) Consequently the Langevin dynamics is unaffected,

$$\mathbf{X}_\mathbf{n}(t + \Delta t) = \mathbf{X}_\mathbf{n}(t) + \frac{\mathbf{f}_\mathbf{n}(t)}{2m_i}\Delta t^2 + \sqrt{k_B T}\, \boldsymbol{\eta}_\mathbf{n}(t)\Delta t, \tag{5.1}$$

where we have introduced the normalized independent Gaussian noise with variance $\langle \boldsymbol{\eta}\boldsymbol{\eta} \rangle = \mathbf{1}$. Because we have established a two-dimensional grid, we may now try to accelerate the dynamics simply by going to Fourier space as described above for a generic lattice field theory. The fields are now the position vectors of each particle. As we will demonstrate numerically in Sec. 6, this grid is indeed useful for a two-dimensional Lennard-Jones fluid.

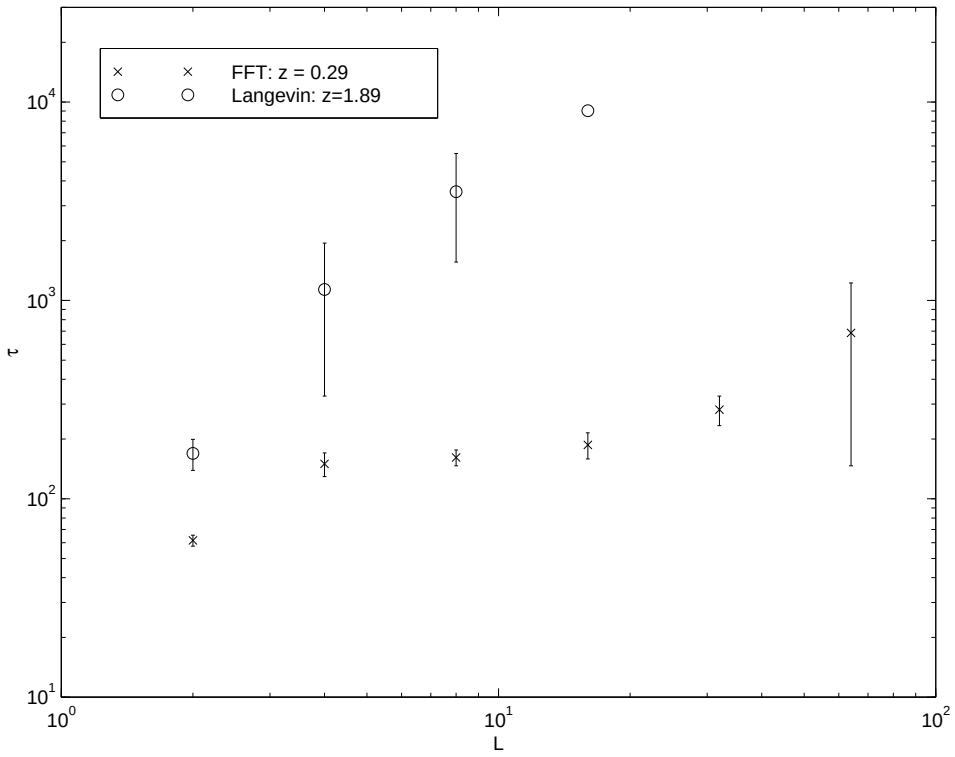

Figure 2: Finite size scaling of the correlation time τ with the linear dimension L for Langevin and FA Langevin simulations of ϕ^4 theory; τ is in units of Δt.

Wavenumber	FAMD		Langevin	
	Value	Error	Value	Error
$n = 1$	12000	$\pm$ 3000	80000	$\pm$ 12000
$n = 2$	3300	$\pm$ 500	22000	$\pm$ 4000
$n = 4$	1100	$\pm$ 130	8600	$\pm$ 600

Table 2: Correlation times in (integration time steps) for different wavelengths for $N = 16$ particles.

6 2D Lennard-Jones Fluid

Motivated by the successful application of Fourier Acceleration to decorrelate lattice ϕ^4 systems, we have tested its ability to reduce the autocorrelation time of a system of Lennard-Jones atoms in two dimensions using the Index Method.

The Lennard-Jones interaction potential is given by

$$V_{LJ}(r) = 4\epsilon \left(\frac{\sigma^{12}}{r^{12}} - \frac{\sigma^6}{r^6} \right). \tag{6.1}$$

In our simulations we chose $\epsilon = \sigma = 1$, a potential cutoff at 2.5σ, and worked at the liquid-vapor critical point, with temperature and density parameters $T = T_c = 0.47$, $\rho_c = 0.35$, respectively. Both pure Langevin MD and FAMD were tested for $N = 16$ and 64 particles with periodic boundary conditions. Each system was evolved on the order of 10^7 integration steps with $\Delta t = 0.005$. This time step allowed us to accurately determine the critical thermodynamic quantities. The acceleration kernel we used in FAMD was identical in form to the one we applied to the ϕ^4 model, namely

$$\epsilon(\mathbf{k}) = \frac{4d + \frac{1}{N}}{4 \sum_{\mu=1}^{d} \sin^2\left(\frac{k_\mu}{2}\right) + \frac{1}{N}} \ (\Delta t)^2 \ , \tag{6.2}$$

where N is now the number of particles in the system. This should be compared to Eq. (4.4).

We allowed the system to evolve for 10^6 steps before statistics were taken. To compare the effectiveness of the Fourier acceleration, we examined the autocorrelation of various long-wavelength modes of the system. In particular, we looked at the circularly averaged time-autocorrelation of the cosine-transformed density. In D spatial dimensions, we write $d\mathbf{k} = k^{D-1} dk \, d\mathbf{\Omega}$, where $k = |\mathbf{k}|$ and $d\mathbf{\Omega}$ is the direction differential, so the cosine-transformed density is

$$\rho(\mathbf{k}, t) = \sum_{i}^{N} \cos(\mathbf{k} \cdot \mathbf{x}_i). \tag{6.3}$$

The autocorrelation that we measure is then

$$A(k, \tau) \equiv \frac{\int d\mathbf{\Omega} \ \rho(\mathbf{k}, t + \tau) \rho(\mathbf{k}, t)}{\int d\mathbf{\Omega}}, \tag{6.4}$$

where $\mathbf{k} = 2\pi \mathbf{n}/L$, and L is the linear dimension of the system.

In Tables 2 and 3, we show the autocorrelation times for various modes in both Langevin and FAMD simulations. As seen from the tables, the FAMD dynamics is clearly more efficient at decorrelating long wavelength modes. A precise measure of the gain over standard Langevin MD was not possible, because standard Langevin MD has a very long correlation time. We therefore do

Wavenumber	FAMD		Langevin	
	Value	Error	Value	Error
$n = 1$	40000	$\pm$ 13000	1200000	$\pm$ 130000
$n = 2$	15000	$\pm$ 2000	310000	$\pm$ 60000
$n = 4$	4200	$\pm$ 700	40000	$\pm$ 4000

Table 3: Correlation times in (integration time steps) for different wavelengths for $N = 64$ particles.

not know exactly how much faster FAMD is. Moreover, whether or not there is simply a decrease in the amplitude of decorrelation time or an actual decrease in its algebraic form is not known. As with the precise determination of z for the ϕ^4-model simulation, that will require considerably more computational effort which we postpone to future work.

Finally, we limited our investigation to a maximum of only 64 particles to allow us to equilibrate the system at its critical point using Langevin dynamics. We expect, that gains over standard Langevin MD will be ever more significant as the number of particles increases, both at and away from the critical point.

7 Discussion

We have described a Fourier-based Langevin scheme, capable of accelerating the dynamics of particulate systems with a Lagrangian data representation. We have demonstrated that there is great potential in speeding up the dynamics of long-wavelength modes. Two issues related to the accelerated dynamics will be addressed in future research. (1) Dynamical faithfulness: how much of the actual dynamics is unchanged by taking different time steps for different wavelength modes? (2) Does this method offer even more of a gain when it is applied to molecular systems with nonconserved order parameters (for example, dipolar systems or systems with structural phase transitions)? We believe that our preliminary computational investigations Fourier methods have shown great promise, and we intend to explore these questions in detail in future work.

Acknowledgements

We thank Harvey Gould, Neils Gronbech-Jensen, and William Klein for very useful discussions. This work was supported in part by NSF grant DMR-9633385, and under the auspices of the Department of Energy at Los Alamos National Laboratory (LA-UR 00-118) under LDRD-DR 98605. BMB was partially supported by AFOSR Grant F49620-95-1-0285.

References

[1] B. Space, H. Rabitz, and A. Askar, *J. Chem. Phys.* **99**, 9070 (1993).

[2] M. E. Tuckerman, B. J. Berne, and A. Rossi, *J. Chem. Phys.* **94**, 1465 (1991).

[3] G. Zhang and T. Schlick, *J. Chem. Phys.* **101**, 4995 (1994).

[4] A. F. Voter, *Phys. Rev. Lett.* **78**, 3908 (1997).

[5] F. A. Bornemann and C. Schuette, *Physica D* **102**, 57–77 (1997).

[6] K. M. Beardmore and N. Gronbech-Jensen, *Phys. Rev. E*, **57** 7278, (1998).

[7] R. H. Swendsen and J.-S. Wang, *Phys. Rev. Lett.*, **58**, 86 (1987).

[8] U. Wolff, *Phys. Rev. Lett.* **62**, 361 (1989).

[9] G. G. Batrouni, G. R. Katz, A. S. Kronfeld, G. P. Lepage, B. Svetitsky, and K. G. Wilson, *Phys. Rev. D* **32**, 2736 (1985).

[10] P. Wesseling, *An Introduction to Multigrid Methods*, J. Wiley, New York (1992).

[11] J. Ambrosiano, L. Greengard, and V. Rokhlin, *Computer Physics Communications* **48**, 117 (1988).

[12] V. B. Shenoy, R. Miller, E. B. Tadmor, D. Rodney, R. Phillips, and M. Ortiz, *J. Mech. Phys. Solids* **47**, 611 (1999).

[13] H. D. Simon, S.-H. Teng, *SIAM Journal on Scientific Computing* **18**, 1436 (1997).

[14] G. G. Batrouni and B. Svetitsky, *Phys. Rev. B* **36**, 5647 (1987).

[15] J. Zinn-Justin, *Quantum Field Theory and Critical Phenomena*, Clarendon Press, Oxford (1996).

[16] R. W. Hockney and J. W. Eastwood, *Computer Simulations Using Particles,* Adam Higler (1988).

[17] A. L. Scheinine, *Phys. Rev. B* **39**, 9368 (1989).

[18] R. Toral in *Third Granada lectures in computational physics: proceedings of the III Granada Seminar on Computational Physics*, Granada, Spain, P. L. Garrido and J. Marro, Springer-Verlag, Berlin (1995).

[19] A. L. Ferreira and R. Toral, *Phys. Rev. E* **47**, R3848 (1993).